CFD Modeling of Gas-Liquid Hydrodynamics in a Stirred Tank Reactor

Gorji, Mahmoud; Bozorgmehry Bozzarjomehry, Ramin*+; Kazemeini, Mohammad
Department of Chemical and Petroleum Engineering, Sharif University of Technology, I.R. IRAN

ABSTRACT: *Multiphase impeller stirred tank reactors enhance mixing of reacting species used in a variety of chemical industries. These reactors have been studied based on Computational Fluid Dynamics (CFD) that can be used in the analysis, design and scale up of these reactors. Most of the researches done in this area are limited to single phase reactors, and a few remaining two phase flow investigations have been done based on MRF (Multi Reference Frame) and Snapshot approach. However, the MRF and snapshot approaches cannot be used in rigorous simulation of unsteady state problems. In order to simulate the unsteady state behavior of the multiphase stirred tank reactors we have used sliding mesh technique to solve the problem rigorously. In this work a 3D CFD model is used to investigate hydrodynamics of a fully baffled cylindrical stirred tank containing air-water in which air is sparged. The tank is equipped with a standard Rushton turbine impeller. This work has been done based on two fluid (Eulerian-Eulerian) model and finite volume method, along with standard k-ε model to address turbulent behavior of both phases. The results obtained for velocity field show a good agreement with the corresponding data published by researchers in this field for the same case. The effect of gas inlet velocity on the gas holds up distribution has been studied. According to the obtained results, there should be an optimum value for gas inlet velocity in order to achieve appropriate gas distribution in the liquid. The most important parameter affecting the optimum value is impeller rotational speed.*

KEY WORDS: *Hydrodynamics, Stirred tank reactor, CFD, Gas-liquid.*

INTRODUCTION

Many examples of gas liquid contacting operations are found in the process industries involving gas incorporation or absorption into liquid, perhaps with chemical reaction in the liquid. This enhances mass transfer operations particularly for cases in which the small solubility of gaseous components in the liquid necessitates a long contact time. (e.g., hydrogenation and oxidation reactions taking place at liquid phase). Therefore, mixing pattern has a significant effect on the performance of the reactor. For low viscosity (say<=0.2 Pa.s), turbulence can be used to obtain good mixing, high interfacial area and high mass and heat transfer coefficients. As an example of equipment enhancing mass transfer operations one can consider mechanically

* *To whom correspondence should be addressed.*
+ *E-mail: brbozorg@sharif.edu*
1021-9986/07/2/85 12/$/3.20

agitated vessels. A suggested configuration for agitated vessel for gas-liquid operation is a cylindrical fully baffled vessel. For this purpose gas is introduced underneath the impeller. The performance of gas-liquid stirred vessels depends on three parameters: vessel size, impeller shape and dimensions and volumetric gas flow rate [1,2]. These parameters in turn affect the gas flow regime, gas hold up distribution, power consumption and gas-liquid mass transfer coefficient. Computational Fluid Dynamics (CFD) is a useful tool to analyze detail of highly complex turbulence flow in mechanically agitated stirred tanks. Most of simulations reported in literature consider only single-phase (liquid) stirred vessels [3-9] and a few of them addresses gas-liquid ones. *Bakker et al.,* [10,11] and *Djebbar et al.,* [12] were the first researchers who worked in this area. They used used IBC (Impeller Boundary Condition) to study the effect of rotating impeller and stationary baffles on fluid mixing.

Moroud et al., used improved IBC method and Eulerian-Elerain model for two phase system and compared the results with laser Doppler Anemometry (LDA) [13]. *Ranade et al.,* have worked on the same problem (i.e., the effect of impeller and baffles on mixing process) using Eulerian-Eulerian model and snapshot method [14]. *Lane et al.,* have studied this problem considering bubble coalescence and break up based on Eulerian-Eulerian model and MRF (Multi Reference Frame) [15]. In another work *Deen et al.,* studied the hydrodynamics of stirred tanks both for single (liquid) phase and two phase (gas-liquid) systems. In their study they used Eulerian-Eulerian model and sliding mesh method in the study of hydrodynamics of two phase stirred tanks. They have compared the results obtained based on their model with experimental results obtained by Particle Image Velocimetry (PIV) [16]. They have also studied the effect of gas on trailing vortices behind impeller.

Khopkar et al., have done a similar study on a stirred tank containing two phase air-water system equipped with a PBT(Pitched Blade Turbine) [17] and standard six blade rushton turbine impeller [18] based on Eulerian-Eulerian model and snapshot method . In the latter work (e.g., rushton turbine impeller system) they compared their simulation results with the corresponding values obtained through (Computer Automated Radioactive Particle Track (CARPT) and Computed Tomography (CT) measurements. *Honkanen et al.,* [19] studied the two phase air-water stirred tank using a different approach based on Volume Of Fluid (VOF) multiphase model and Large Eddy Simulation (LES) method to model turbulence behavior of the system. They studied the velocity field but had no study on gas hold up distribution.

Most of these studies utilized Impeller Boundary Condition (IBC) which needs experimental velocity data for impeller region and Multi Reference Frame (MRF) or snapshot method. These techniques require less computational resources comparing to sliding mesh method. Therefore the MRF method is faster than sliding mesh method. However the higher speed is achieved at the expense of accuracy. Hence, in order to obtain more accurate results one should use sliding mesh technique. In this work the hydrodynamics of a fully baffled cylindrical stirred tank equipped with a six blade standard rushton turbine impeller for a two phase (air-water) system has been studied. In order to study the effect of rotating impeller and stationary baffles on the hydro-dynamics of the system, authors have used Eulerian-Eulerian model and sliding mesh method along with k-ε method to present turbulence of both phases. The results obtained in this work have been compared with those reported by *Khopkar* [18]. Due to high difference between air and water volatility, the effect of phase equilibrium on the behavior of the system has been neglected.

DEVELOPMENT OF CFD MODEL

Mathematical Modeling

The Navier-Stockes Equations and Turbulence Modeling

To model the hydrodynamic behavior of the gas-liquid system in the stirred vessel, a two-fluid or Eulerian-Euerian approach has been used, where the gas and liquid phase are considered as interpenetrating continua for which the continuity and momentum equations are solved. The ensemble averaged mass and momentum balance (Navier-Stockes equations) for each phase may be written as:

$$\frac{\partial(\alpha_k \rho_k)}{\partial t} + \nabla \cdot (\alpha_k \rho_k U_k) = 0 \quad (1)$$

$$\frac{\partial(\alpha_k \rho_k U_k)}{\partial t} + \nabla \cdot (\alpha_k \rho_k U_k U_k) = \quad (2)$$

$$-\alpha_k \nabla P + \nabla \cdot (\alpha_k \tau_k) + \alpha_k \rho_k g + F_{kl}$$

Where U_k is the velocity of phase k and F_{kl} is the inter-phase momentum exchange term between phases 'k'and 'l', and τ_k is the stress tensor for phase k described by equation (3):

$$\tau_k = \mu_k(\nabla U_k + \nabla U_k{}^T) - \frac{2}{3}\mu_k \nabla.U_k I \quad (3)$$

The standard k-ε model is used for both phases. The equations for turbulent kinetic energy, k, and turbulent kinetic energy dissipation rate, ε, are as follows [20,21]:

$$\frac{\partial(\alpha_k \rho_k k)}{\partial t} + \nabla.(\alpha_k \rho_k U_k k) = \quad (4)$$

$$\nabla.(\alpha_k \frac{\mu_t}{\sigma_k}\nabla k) + \alpha_k(G - \rho_k \varepsilon)$$

$$\frac{\partial(\alpha_k \rho_k \varepsilon)}{\partial t} + \nabla.(\alpha_k \rho_k U_k \varepsilon) = \quad (5)$$

$$\nabla.(\alpha_k \frac{\mu_t}{\sigma_\varepsilon}\nabla k) + \alpha_k \frac{\varepsilon}{k}(C_1 G - C_2 \rho_k \varepsilon)$$

$$G = \mu_k(\nabla U_k + \nabla U_k{}^T) : \nabla U_k \quad (6)$$

$$\mu_t = \rho_k c C_\mu \frac{k^2}{\varepsilon} \quad (7)$$

Where G is turbulence generation rate and μ_t is turbulent viscosity. The parameters used in standard k-ε model for both liquid and gas phases are as follows: C_μ=0.09, C_1=1.44, C_2=1.92, σ_k=1.0 and σ_ε=1.3.

For more information regarding governing equations, one can refer to *Ranade's* work [20].

Interaction Forces

The inter-phase momentum exchange term consists of four terms: the *Basset* force, the virtual mass force, the lift force and the inter-phase drag force. In the bulk region of vessel, the velocity gradients are not large. Near the impeller, pressure gradients and inter-phase drag forces mainly dominate the motion of bubbles. An order of magnitude analysis indicates that the magnitude of the lift force is much smaller than inter-phase drag force [17]. Recent numerical experiments reported by *Khopkar et al.,* indicate that the effect of virtual mass force is not significant in the bulk region of stirred vessel [17]. In most cases, the magnitude of *Basset* force is also much smaller than that of the inter-phase drag force [18].

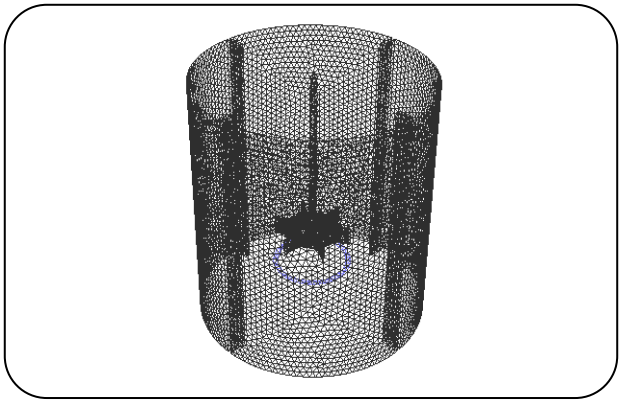

Fig. 1: Vessel geometry and grid generation.

Therefore, the only force that should be considered as the interaction force in the inter-phase momentum exchange for this specified case is the drag force. The inter-phase drag force is defined by equation (8):

$$F_{kl} = \frac{3}{4}\rho_L \alpha_G \frac{C_D}{d_b}|U_L - U_G|(U_L - U_G) \quad (8)$$

Where C_D is calculated from *Schiller-Nauman* correlation [20]:

$$C_D = \frac{24}{Re_G}(1 + 0.15 Re_G{}^{0.687}) \quad ; \quad Re_G \le 1000 \quad (9)$$

$$C_D = 0.44 \quad ; \quad Re_G > 1000 \quad (10)$$

$$Re_G = \frac{\rho_L d_b |U_G - U_L|}{\mu_L} \quad (11)$$

VESSEL GEOMETRY AND GRID GENERATION

The tank geometry employed in this work is a flat bottom fully baffled cylindrical tank, whose diameter and height are T=0.20 m, H=0.20 m, respectively (Fig. 1). Four equally spaced baffles, whose width is one tenth of tank diameter (b=T/10) have been mounted perpendicular to the vessel wall. A standard (six blade) Rushton turbine impeller's whose diameter, blade height and width are D=T/3, B=D/4, W=D/5, respectively. The impeller is installed along the axis of the tank with a shaft diameter of ds=0.003 m and an off-bottom clearance of C=T/3. The impeller rotates at a speed of 200 rpm which corresponds to impeller *Reynolds* number of, Re=14800. Air is sparged into the vessel through a ring sparger of inner and outer diameter 30, 34 mm, respectively. The height of sparger ring is 4 mm and is located at a distance

of T/6 from the bottom of the vessel. The quadratic upstream interaction for convective kinetics (QUICK) has been used for discreization. In this work sliding mesh approach has been considered to study unsteady state behavior of the system's hydrodynamics.

In this approach, the whole vessel is divided in two regions: an inner region attached to the rotating impeller and shaft; and outer region attached to the stationary baffles and the vessel. The inner and outer regions meet each other at an interface positioned at r=0.065 m, and $0.04<z<0.14$ m and $0\leq\theta\leq2\Pi$. The tank was modeled by a finite volume grid in cylindrical coordinate with 374912 cells ($r\times\theta\times z$: $58\times101\times64$). The grid number selected by researchers in the same case of two phase stirred tank vessel has been reviewed [15,18,20,22]. The effect of the number of cells and grid resolution has also been checked and it was found that use of finer mesh has no effect on the results. The time step used in the simulation is 0.005 sec. Despite the fact that small time step results in a long tie for simulation, it can not get larger because it severely deteriorates the accuracy of the results.

BOUNDARY CONDITION AND FLUID PROPERTIES

In this work, the upper side of sparger from which air is sparged, has been modeled as an inlet velocity boundary condition. It is assumed that pure air with a velocity of 0.1, 0.5 m/sec is entering into the system at this boundary. Other sides of sparger are modeled as solid walls. The tank is filled with water up to level of 0.195 m and the remaining space contains air. No slip boundary conditions are imposed on all walls and they are introduced to the calculation via standard wall functions. The top surface of liquid has been considered to be flat. In a gas-liquid stirred vessel, there may be a wide distribution of bubble size.

The prevailing bubble size distribution in a gas-liquid stirred vessel is controlled by several parameters such as vessel and sparger configuration, impeller speed and gas flow rate. It is seen that bubbles are largest in high gas fraction plume leading from the sparger to the impeller. In the impeller discharge smaller bubbles are generated due to break up in the highly turbulent impeller discharge stream, while above and below the impeller stream the bubbles become larger again due to coalescence. This pattern has been reported by *Lane et al.*, [15]. Their experimental results showed that bubble size in the bulk of the tank is generally in the range of 3 to 4 mm. It is possible to develop a detailed multi-fluid computational model using the population balance framework to account for bubble size distribution. *Buwa* and *Ranade* [23] and *Rafique et al.*, [24] developed and validated such a model for gas-liquid flow in bubble columns.

However, use of multi-fluid models based on population balances increases computational demands. Moreover, available experimental data for bubble size distribution in stirred vessel is not sufficient to calculate the certain parameters appearing in coalescence and break up kernels. Apart from the uncertainty in parameters of coalescence and break up kernels, there is a significant uncertainty in estimation of inter-phase drag force on gas bubbles in presence of other bubbles and high levels of turbulence prevailing in the vessel [18]. Therefore, using a multi-fluid model for stirred tank is not applicable due to inability to measure the bubble size distribution in the stirred tank [18].

Barigou and *Greave* [25] reported experimentally measured bubble size distribution for the stirred vessel of 1m diameter (with H=T=1m,C=T/4 and D=T/3). Their experimental data clearly indicates that the bubble sizes in the bulk region of the vessel vary between 3.5 and 4.5 mm at the high gas flow rate. In another research *Gosman et al.*, [26] used 4 mm diameter air bubbles in a air-water stirred tank system of 0.915 m diameter and indicated that despite the fact that assuming a uniform bubble dose not seem to be realistic due to bubble break up and coalescence, using a constant bubble size around 4 mm does not have a major effect on the simulation results. Considering these issues; it is assumed that no coalescence and break up of bubbles exists and a single bubble size of 4 mm has been used in the present work. Fluid properties have been set to those of water and air for primary and secondary phases, respectively.

IMPELLER BOUNDARY CONDITION

The interaction of rotating impeller and the stationary baffles in baffled stirred reactors generate a complex three dimensional flow pattern. This flow has been modeled by employing several different approaches which can be classified into four types: Impeller Boundary Condition (IBC) or block box diagram, Multiple Reference Frame (MRF) or inner-outer

approach, snapshot approach and sliding mesh approach. Ranade has reviewed various approaches for simulating the flow in baffled stirred tank [20]. Most flow simulations of stirred vessels published before 1997 were based on steady state analysis using IBC approach. In this approach the impeller is not directly simulated and therefore requires boundary conditions on the impeller swept surface, which need to be determined experimentally.

Although this approach is reasonably successful in predicting the flow characteristics in the bulk of the vessel, its use is inherently restricted to cases for which experimental data is available. Moreover, this approach does not provide information about the flow in the impeller region. Extension of such an approach to multiphase flows and to industrial-scale reactors is not feasible because it is virtually impossible to obtain accurate boundary conditions for such systems by experimental measurements. To eliminate some of the limitations described above, attempts have been made to develop an approach which allows a priori simulations of the flow field generated by an impeller of any shape. There are two main approaches for approximating unsteady flow in stirred vessels via steady state simulations.

In both approaches the whole solution domain is divided into two regions using a fictitious cylindrical zone with a radius more than that of the impeller blade tip and less than that of the inner edges of the baffles. The height of this fictitious zone should be such that it contains the entire impeller.

The full geometry needs to be modeled and impeller blades are modeled as walls. In the first approach, flow characteristics of the inner region are solved using a rotating framework. Then the results obtained for this zone are used to provide boundary conditions for outer region (after azimuthally averaging) in which flow field is solved based on a stationary framework. Solution of the outer region is used to obtain the boundary conditions for the inner region. After going through a few iterations between inner and outer regions the iterative procedure might converge to the correct solution. Multi Reference Frame proposed by *Lou et al.,* [27] and Inner-Outer method proposed by *Brucato et al.*, [28] are using this approach [20].

The second approach called snapshot method is based on taking a snapshot of flow in stirred vessels with a fixed relative position of blades and baffles. In this approach impeller blades are modeled as solid walls and flow is simulated using a stationary framework for a specific blade position. Appropriate sources are specified to simulate impeller rotation. If necessary, simulations are carried out at different blade positions to obtain ensemble-averaged results over different blade positions. In the inner region surrounding the impeller, time derivative terms are approximated in terms of spatial derivatives. In the outer region, time derivative terms are neglected [18,20,29]. It should be noted that these two approaches are appropriate in nature.

In order to obtain the exact solution of the flow problem, *Lou et al.,* [30] proposed the sliding mesh technique in which the full transient simulations are carried out. In this method the whole solution domain is divided into two non-overlapping inner and outer grid zones. Obviously, the boundary between these two zones should have a radius more than that of the impeller blade and less than that of the inner edges of the baffles and a height sufficient to include the entire impeller.

The detailed geometry of the impeller needs to be modeled for which impeller blades are modeled as solid rotating walls. The two mesh zones interact along a common grid interface. The outer grid zone is attached to the stationary baffles and reactor wall while the inner is attached to the rotating impeller and is allowed to rotate stepwise. The moving grid is allowed to slide relative to stationary one and grid lines are not required to align on the common surface.

This makes it possible to have an exact model for the impeller and baffles. Flow within the impeller blades is solved and recalculated for each time step using the usual transport equations without any simplification in time derivative terms unlike the previous methods. Two regions are implicitly coupled at the interface via a sliding mesh algorithm. This approach has a priori predictions without requiring any experimental input. It can therefore be used as a design tool to screen different configurations.

Since sliding mesh technique is computationally intensive, there are some restrictions on the number of meshes of computational cells that can be used for simulation purposes [20,30,31]. In this paper, sliding mesh method technique has been used due to its rigor and generality.

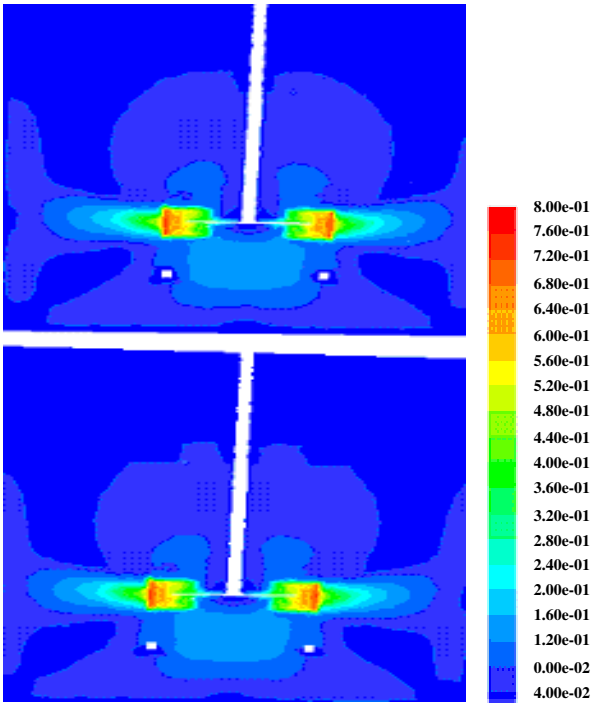

Fig. 2: Contours of air (bottom) and water (top) velocity in mid-baffle plane (air inlet velocity of 0.1m/sec, impeller rotational speed of 200 rpm).

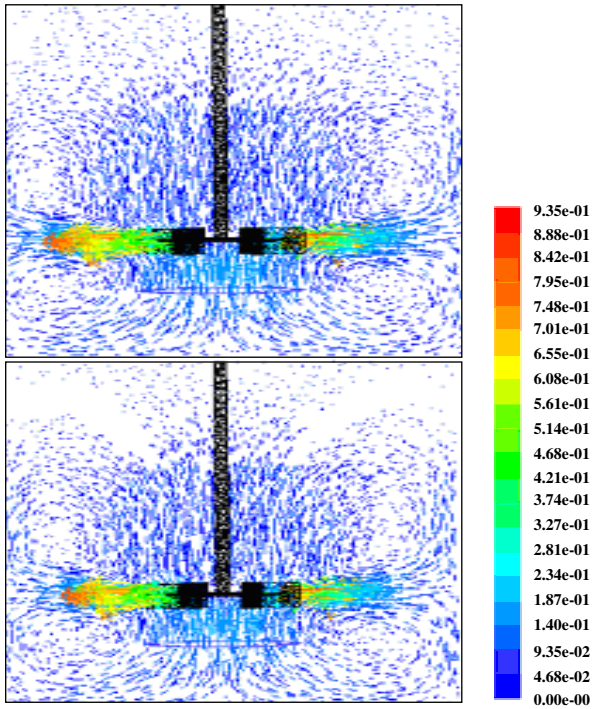

Fig. 3: Vectors of water (first) and air (second) velocity in mid-baffle plane (air inlet velocity of 0.1m/sec, impeller rotational speed of 200 rpm).

RESULTS AND DISCUSSION

The selected bench mark described in previous section is the same one studied by *Khopkar* [18]. This bench mark has been simulated at two different air velocities of 0.1 and 0.5 m/sec at a fixed impeller speed of 200 rpm which leads to impeller *Reynolds* number of Re=14800. Hydrodynamics behavior of the system has been dynamically simulated from its initial condition in which liquid is at rest. In addition, influence of air inlet velocity on the bubble hold up in liquid has been studied. Unfortunately, very limited experimental data is available to make systematic comparison of simulation results and the corresponding experimental data. Even for those limited cases where data is available, a complete set of data, that is gas and liquid phase velocity along with gas volume fractions, is not available for the same vessel geometry. Therefore, we have validated the simulation by comparing the results with the corresponding data published for the same bench mark in a qualitative manner [14,15,22]. The same approach used by *Ciofalo et al.*, [32] and *Brucato et al.,* [33].

Figs. 2 to 4 show the liquid and gas velocities; and distribution of gas hold up of air at the mid-baffle plane corresponding to air inlet velocity of 0.1 m/sec about 5.9 sec after startup. The liquid phase velocity simulation results obtained in this work are compared against similar results reported by *Khopkar* [18] in Fig. 6. Comparison shows that the results are almost the same. Fig. 5 shows absolute pressure of air-water mixture (contour of mixture absolute pressure) in impeller center plane corresponding to the same air inlet velocity and time. According to this figure, pressure behind impeller blades is less than its value in front of blades in which impeller rotates in clockwise direction. This issue has been obtained by other researchers as well [15,18].

Velocity Fields

The predicted liquid velocity fields obtained through simulation show the upward inclination of impeller discharge stream in the presence of gas which is in agreement with the results obtained and reported by other researchers [14,18]. Results show that at low air inlet velocity, the global liquid and gas flow pattern are roughly the same as the ones encountered for the single-phase flow of liquid. The gas phase flows more or less in the similar manner that the liquid does, and presence of

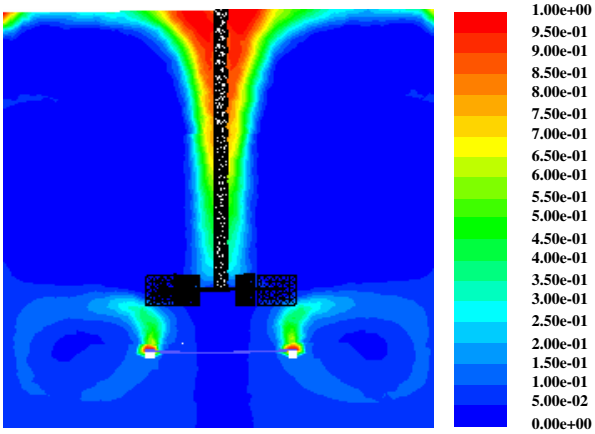

Fig. 4: Contour of air volume fraction in mid-baffle plane (air inlet velocity of 0.1m/sec, impeller rotational speed of 200 rpm).

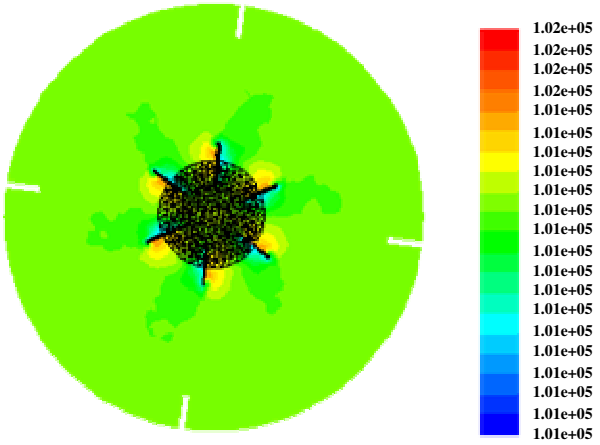

Fig. 5: Contour of air and water mixture pressure (Pa) in impeller center plane (air inlet velocity of 0.1m/sec, impeller rotational speed of 200 rpm).

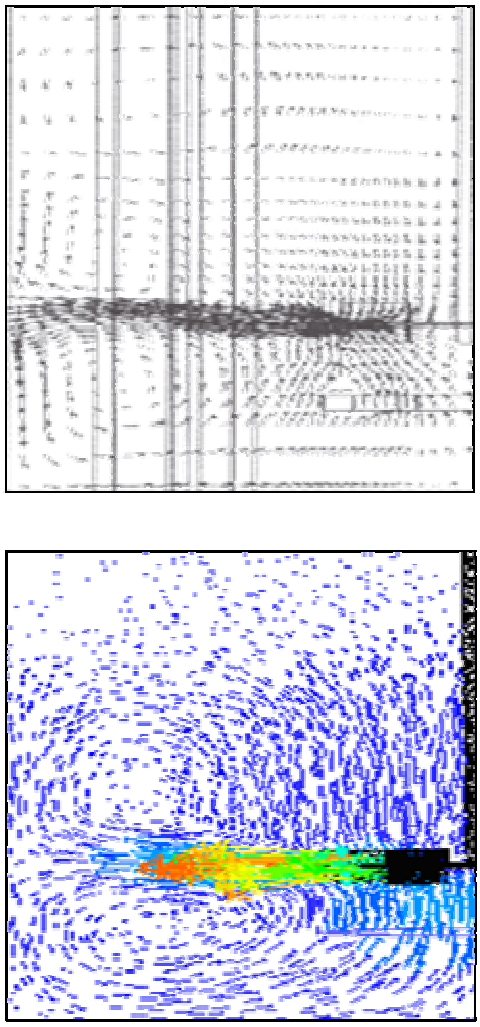

Fig. 6: Comparison of obtained vector of water velocity in mid-baffle plane(second) with Khopkar result (first) [18] at impeller rotational speed of 200 rpm.

gas only slightly changes the flow field obtained in a single-phase system. It can be explained considering the fact that the inlet air velocity is much lower than the radial velocity imposed by the mixing device. In order to show the effect of rising gas on the upward inclination of the radial jet emerging from the impeller discharge stream, the velocity fields in the system have been shown for two different air inlet velocities of 0.1 m/sec and 0.5 m/sec in Figs. 3 and 9, respectively. Comparing these figures shows that by increasing air inlet velocity, inclination of impeller discharge stream increases. It was also observed by *Khopkar et al.*, [18] that increase in gas flow increases upward inclination of impeller discharge stream. Apart from upward inclination of impeller discharge stream, the predicted gas flow field and gas hold up distribution in Figs. 3 and 4 show the inward movement of the gas. This inward movement of rising gas generates the secondary circulation of liquid in the upper region of the vessel because the liquid is dragged upward by the gas bubbles. Figs. 7 to 9 show the distribution of gas hold up; and liquid and gas velocities in the mid-baffle plane corresponding to air inlet velocity of 0.5 m/sec about 4 sec after startup. Comparing Figs. 3 and 9 show that by increasing the air inlet velocity, the inward movement of rising gas increases. The observed inward movement of the gas was also seen to be very

strong in the higher gas flow rates by *Khopkar* [18]. The comparison also shows that at low air inlet velocity, the flow pattern induced by the impeller is less distributed by the gas flow, whereas at higher air inlet velocity the gas flow has significant effect on the flow pattern and system hydrodynamics and increases the intensity of the circulating flow. Fig. 10 shows the volume averaged velocity of gas and liquid phase as a function of time for impeller rotational speed of 200 rpm and air inlet velocities of 0.8 and 1 m/sec, respectively. The figure shows that the averaged gas and liquid velocities have the unsteady state behavior up to about 0.9 sec after start up, of the system at which the steady state condition is established.

Gas Hold up Distribution

Figs. 4 and 7 represent gas hold up distribution throughout the tank for air inlet velocity of 0.1 and 0.5 m/sec, respectively. Fig. 4 shows that bubbles rise from the sparger and are pushed toward the vessel wall because inlet air velocity (0.1 m/sec) is much lower than the radial velocity (0.7 m/sec) imposed by the mixing device. Comparing Figs. 4 and 7 show that at low inlet air velocity the gas bubbles are dispersed in lower circulation loop and is not well distributed throughout the liquid, whereas at higher air inlet velocity gas bubbles are dispersed in both circulation loops above and below the impeller. Therefore, increasing the air inlet velocity results in more appropriate gas distribution in the liquid. This issue has been reported by *Ranade et al.,* [19] on a similar system whose diameter is 0.3 m. They showed that the gas bubbles rise from the sparger and are transported radially outward by the impeller stream. Furthermore, according to the results reported by *Lane et al.,* [15] on a similar system with a diameter of 1 m, the gas rises up to the impeller and then is dispersed throughout the bulk of the liquid.

Figs. 11 and 12 show distribution of air hold up in the impeller center plane corresponding to air inlet velocity of 0.8 and 1 m/sec, 0.8 and 0.6 sec after start up, respectively. As previously mentioned, the impeller rotates clockwise. According to these figures, the gas accumulation takes place behind the impeller blades which is explained by the low pressure zones existing at these locations. This issue has also been reported by researchers who worked on the similar problem both in

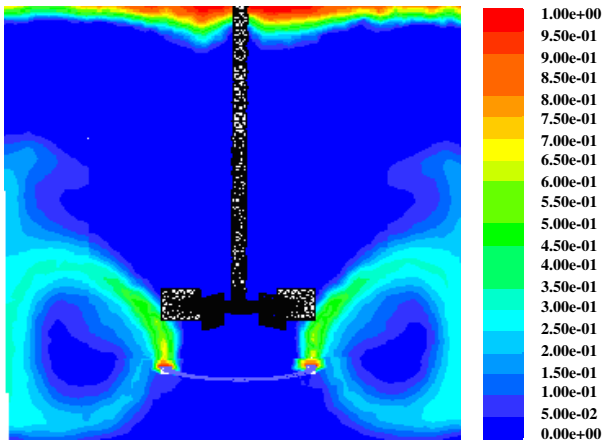

Fig. 7: Contour of air volume fraction in mid-baffle (air inlet velocity of 0.5 m/sec, impeller rotational speed of 200 rpm).

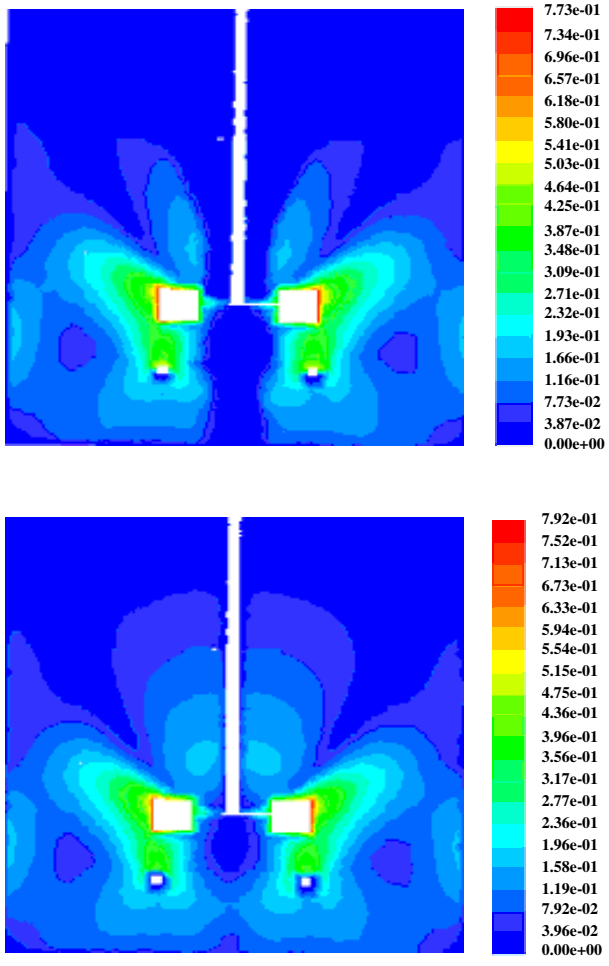

Fig. 8: Contours of air (top) and water (bottom) velocity in mid-baffle plane (air inlet velocity of 0.5 m/sec, impeller rotational speed of 200 rpm).

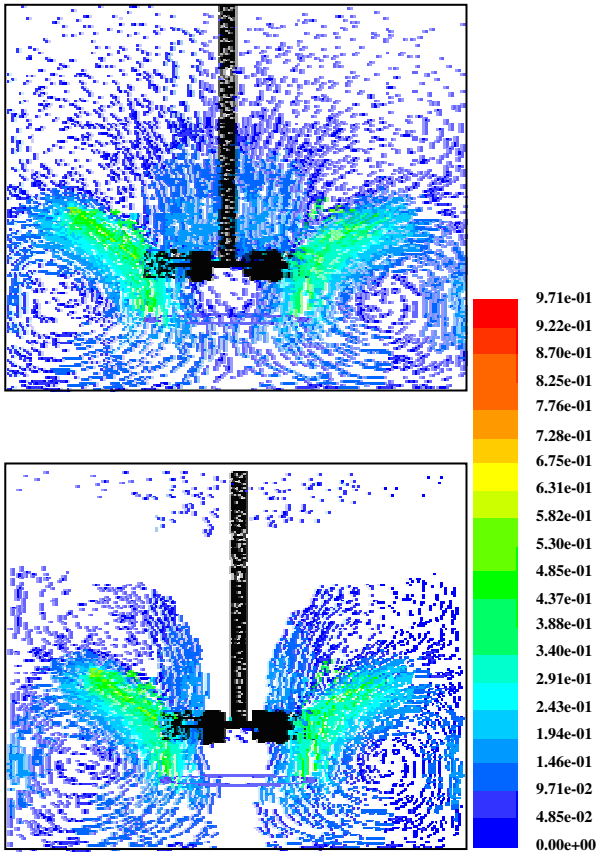

Fig. 9: Vectors of air (bottom) and water (top) velocity in mid-baffle plane (air inlet velocity of 0.5 m/sec, impeller rotational speed of 200 rpm).

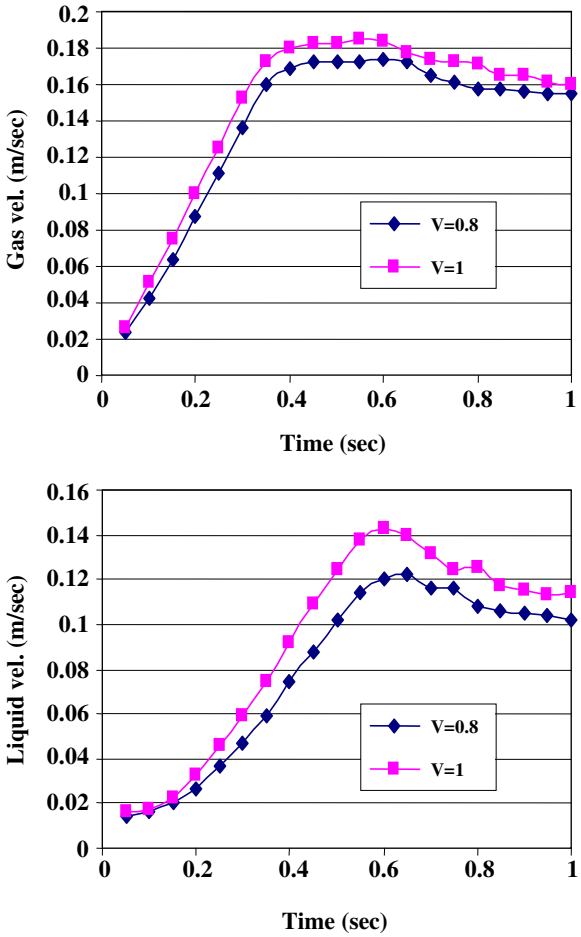

Fig. 10: Comparison of volume averaged liquid and gas velocities versus start up time for air inlet velocities of 0.8 and 1 m/sec (impeller rotational speed of 200 rpm).

experimental and simulation studies [14, 18, 22]. Fig. 13 shows the volume averaged gas hold up at air inlet velocities of 0.8 and1 m/sec. The figure shows temporal increment of gas hold up as a function of time.

On the other hand as Fig. 14 shows increase of gas inlet velocity beyond a certain threshold deteriorates gas distribution in the liquid because it flows in an upward straight path as if there is no impeller in the vessel. Hence, for gas-liquid stirred tank reactors at which a set of reactions between gas and liquid are taking place, one should use a judicious (if not optimum) value for gas inlet velocity in order to enhance the performance of the reactor.

However, the optimum value for the gas inlet velocity depends on both the reaction kinetics and mechanical design of the stirred tank (e.g., vessel size; impeller shape, dimension, rotational speed and position).

CONCLUSIONS

Hydrodynamics of air-water system in a fully baffled stirred vessel with a standard six blade rushton turbine impeller has been investigated using sliding mesh method to account for relative movement of rotating impeller and stationary baffles. For impeller rotational speed of 200 rpm and air inlet velocity of 0.1, 0.5 m/sec, flow field of liquid and gas phase generated by the impeller and gas hold up distribution in the vessel have been obtained. The computational model correctly captured the overall flow field generated by a standard rushton turbine, including the two circulation loops above and below the impeller. Apart from the presence of two circulation loops above and below impeller, the predicted liquid velocity fields show the upward inclination of jet issuing from the impeller discharge stream in the presence of the gas. This is in agreement with the published experimental

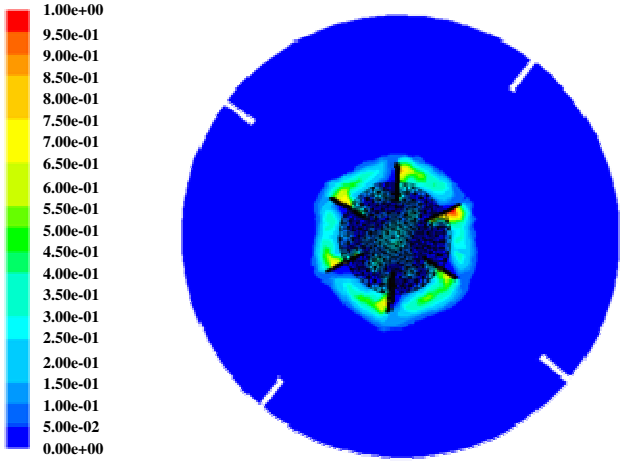

Fig. 11: Contour of air volume fraction in impeller center plane (impeller rotational speed of 200 rpm and air inlet velocity of 0.8 m/se @ 0.8 sec after start up).

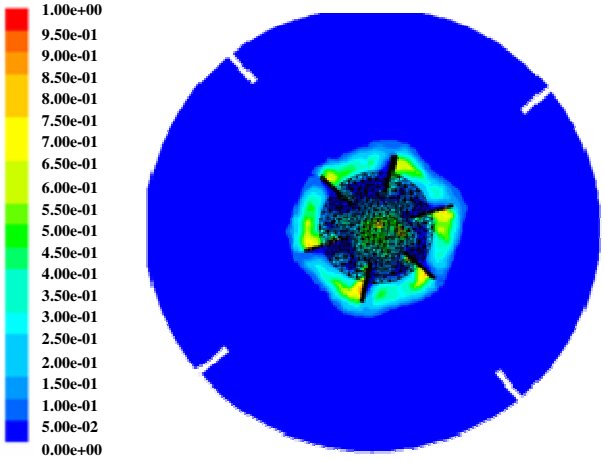

Fig. 12: Contour of air volume fraction in impeller center plane (impeller rotational speed of 200 rpm and air inlet velocity of 1m/se @ 0.6 sec after start up)

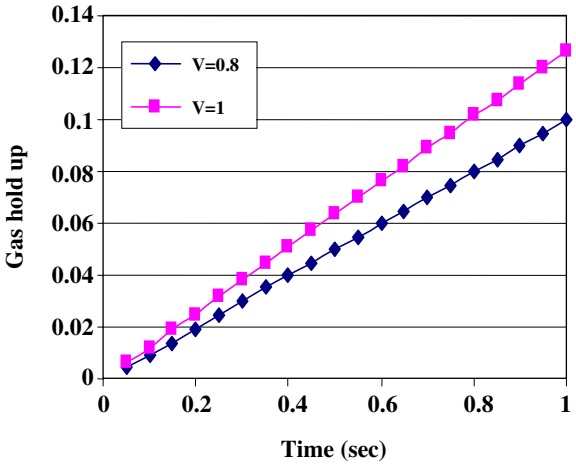

Fig. 13: Comparison of volume averaged gas holdup versus start up time for air inlet velocities of 0.8 and 1 m/sec (impeller rotational speed of 200 rpm).

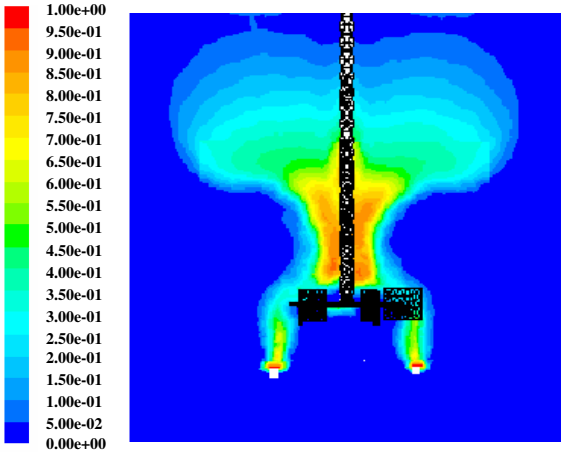

Fig. 14: Contour of air volume fraction in mid-baffle plane (impeller rotational speed of 200 rpm and air inlet velocity of 1m/se @ 0.42 sec after start up).

evidence. Results show that increasing air inlet velocity results in upward inclination of impeller discharge stream. These results obtained by simulation have been validated also with the corresponding results for the same bench mark reported by *Khopkar et al.*, [18].

The study shows that at low inlet air velocity compared to impeller tip speed, the air is pushed toward the vessel wall due to higher impeller radial speed compared to air rising velocity. In this case the gas bubbles circulate below the impeller and the amount of gas at the bottom of the tank is high. The gas hold up and velocity distribution show that increasing the air inlet velocity results in better gas distribution throughout the liquid. On the other hand increase of gas inlet velocity beyond a certain threshold deteriorates gas distribution in the liquid because it flows in an upward straight path as if there is no impeller in the vessel. Hence for a constant impeller speed and specified tank geometry there is an optimum value for inlet gas velocity at which maximum gas distribution in the liquid is achieved. This is a very important factor in the design of gas-liquid stirred tank reactors. The optimum value of this factor depends on both mechanical design (geometry and impeller speed) and kinetic of reactions taking place in the reactor.

Received : 24th September 2005 ; Accepted : 9th October 2006

REFERENCES

[1] Harnby, N., Edwards, N.F., Nienow, A.W., "Mixing in Process Industries", McGraw-Hill (1985).

[2] Tatterson, G.B., "Fluid Mixing and Gas Dispersion in Agitated Tanks", McGraw-Hill, New York (1991).

[3] Aubin, J., Fletcher, D.F., Xuereb, C., Modeling Turbulent Flow in Stirred Tanks with CFD: The Influence of Modeling Approach, Turbulence Model and Numerical Scheme, *Experimental Thermal and Fluid Science*, **28**, 431 (2004).

[4] Bujalski, W., Jaworski, Z., Nienow, A.W., CFD Study of Homogenization with Dual Rushton Turbines-Comparision with Experimental Results-part II: The Multiple Reference Frame, *Transactions of the Institution of Chemical Engineers*, **80**, 97 (2002).

[5] Jaworski, Z., Dyster, K. N., Nienow, A. W., The Effect of Size, Location and Pumping Direction of Pitched Blade Turbine Impellers on Flow Patterns: LDA Measurements and CFD Predictions, *Transactions of the Institution of Chemical Engineers*, **79**, 887 (2001).

[6] Mavros, P., Mann, R., Vlaev, S.D., Bertrand. J., Experimental Visualization and CFD Simulation of Flow Ptterns Induced by a Novel Energy-Saving Dual-Configuration Impeller in Stirred Vessels, *Transactions of the Institution of Chemical Engineers*, **79**, 857 (2001).

[7] Micale, G., Brucato, A., Grisafi, F., Ciofalo, M., Prediction of Flow Fields in Dual-Impeller Stirred Vessel, *A.I.Ch.E. Journal*, **45**, 445 (1999).

[8] Murthy Shekhar, S., Jayanti, S., CFD Study of Power and Mixing Time for Paddle Mixing in Unbaffled Vessels, *Transactions of the Institution of Chemical Engineers*, **80**, 482 (2002).

[9] Ng., K., Fentiman, N.J., Lee, K.C., Yianneskis, M., Assessment of Sliding Mesh CFD Predictions and LDA Measurements of the Flow in a Tank Stirred by a Rushton Impeller, *Transactions of the Institution of Chemical Engineers*, **76**, 737 (1998).

[10] Bakker, A., Hydrodynamics of Stirred Gas-Liquid Dispersions, Ph.D. Thesis, Delf University of Technology, Netherlands (1992).

[11] Bakker, A., van der Akker, H.E.A., A Computational Model for the Gas-Liquid Flow in Stirred Reactors, *Transactions of the Institution of Chemical Engineers*, **72**, 594 (1994).

[12] Djebbar, R., Roustan, M., Line, A., Numerical Computation of Gas-Liquid Dispersion in Mechanically Agitated Vessels, *Transactions of the Institution of Chemical Engineers*, **74**, 492 (1996).

[13] Morud, K.E., Hjertager, B.H., LDA Measurements and CFD Modeling of Gas-liquid Flow in Stirred Vessel, *Chemical Engineering Science*, **51**, 233 (1996).

[14] Ranade, V.V., Deshpande, V.R., Gas-Liquid Flow in Stirred Reactors: Trailing Vortices and Gas Accumulation Behind Impeller Blades, *Chemical Engineering Science*, **54**, 2305 (1999).

[15] Lane, G.L., Schwarz, M.P., Evans, G.M., Predicting Gas-Liquid Flow in a Mechanically Stirred Tank, *Applied Mathematical Modeling*, **26**, 223 (2002).

[16] Deen, N. G., Solberg, T., Hjertager, B. H., Flow Generated by an Aerated Rushton Impeller: Two Phase PIV Experiments and Numerical Simulations, *The Canadian Journal of Chemical Engineering*, **80**, 1 (2002).

[17] Khopkar, A.R., Aubin J., Xureb, C., Le Sauze, N., Ertrand, J., Ranade, V.V., Gas-Liquid Flow Generated by a Pitch Blade Turbine: PIV Measurements and CFD Simulations, *Industrial and Engineering Chemistry and Research*, **42**, 5318 (2003).

[18] Khophkar, A. R, Rammohan, A. R., Ranade, V. V., Dudukovic, M.P., Gas-Liquid Flow Generated by a Rushton Turbine in Stirred Tank Vessel: CAPRT/CT Measurements and CFD Simulations, *Chemical Engineering Science*, **60**, 2215 (2005).

[19] Honkanen, M., Koohestani, A. , Hatunen, T., Saarenrinne, P., Zamankhan, P., Large Eddy Simulation and PIV Experiments of a Two Phase Air-Water Mixer, ASME Fluid Engineering Summer Conference, June,19-23, Houston (2005).

[20] Ranade, V. V, Computational Flow Modeling for Chemical Reactor Engineering, Academic Press, New York (2002).

[21] Versteeg, H. K., Malalasekera, W., An Introduction to Computational Fluid Dynamics, Addison Wesley Longman Limited, New York (1996).

[22] Gentric, C, Mignon, D., Bousquet, J., Tanguy, P.A., Comparison of Mixing in Two Industrial Gas-Liquid Reactors Using CFD Simulations, *Chemical Engineering Science*, **60**, 2253 (2004).

[23] Buwa, V. V., Ranade, V. V., Dynamics of Gas-Liquid Flow in Rectangular Bubble Columns, *Chemical Engineering Science*, **57**, 4715 (2002).

[24] Rafique, M., Chen, P., Dudokovic, M.P., Computational Modeling of Gas-Liquid Flow in Bubble Columns, *Reviews in Chemical Engineering*, **20**, 225 (2004).

[25] Barigou, M., Greaves, M., Buuble Size Distribution in a Mechanically Agitated Gas-Liquid Contactor, *Chemical Engineering Science*, **47**, 2009 (1992).

[26] Gosman, A.D., Lekakou, C., Politis, S., Issa, R.I., Looney, M.K., Multi-dimensional Modeling of Turbulent Two Phase Flow in Stirred Vessels, *A.I.Ch.E. Journal*, **38**, 1947 (1992).

[27] Luo, J. Y., Gosman, A. D., Prediction of Impeller-Induced Flow in Mixing Vessels Using Multiple Frames of Reference, Institution of Chemical Engineering Symposium Series, **136**, 549 (1994).

[28] Brucato, A., Ciofalo, M., Grisafi, F., Micale, G., Complete Numerical Simulation of Flow Fields in Baffled Stirred Vessels: The Inner-Outer Approach, Institution of Chemical Engineering Symposium Series, **1360**, 155 (1994).

[29] Ranade, V.V., van den Akker, H.E.A., A Computational Snapshot of Gas-Liquid Flow in Baffled Stirred Reactors, *Chemical Engineering Science*, **49**, 5175 (1994).

[30] Luo, J.Y., Gosman, A.D., Issa, R.I., Midelton, J.C. and Fitzgerald, M.K., Full Flow Field Computation of Mixing in Bafeled Stirred Vessels, *Chemical Engineering Reserch and Design*, **71**(A), 342 (1993).

[31] Montante, G., Lee, K.C., Brucato, A., Yianneskis, M., Numerical Simulations of the Dependency of Flow Pattern on Impeller Clearance in Stirred Vessel, *Chemical Engineering Science*, **56**, 3351 (2001).

[32] Ciofalo, M., Brucato, A., Grisafi, F., Tocco, R., Turbulent Flow in Closed and Free-Surface Tanks Stirred by Radial Impeller, *Chemical Engineering Science*, **51**, 3557 (1996).

[33] Brucato, A., Ciofalo, M., Grisafi, F., Tocco, R., On the Simulation of Stirred Tank Reactors Via Computational Fluid Dynamics, *Chemical Engineering Science*, **55**, 291 (2002).